

Suppression of stimulated Brillouin scattering in optical fibers using a linearly chirped diode laser

J. O. White,^{1,*} A. Vasilyev,² J. P. Cahill,¹ N. Satyan,² O. Okusaga,¹ G. Rakuljic,³ C. E. Mungan,⁴ and A. Yariv²

¹ U.S. Army Research Laboratory, 2800 Powder Mill Road, Adelphi, Maryland 20783, USA

² Department of Applied Physics and Materials Science, California Institute of Technology, 1200 E. California Blvd. 136-93, Pasadena, California 91125, USA

³ Telaris, Inc., 2118 Wilshire Blvd. #238, Santa Monica, California 90403, USA

⁴ Physics Department, U.S. Naval Academy, Annapolis, Maryland 21402, USA

*jeffrey.owen.white@us.army.mil

Abstract: The output of high power fiber amplifiers is typically limited by stimulated Brillouin scattering (SBS). An analysis of SBS with a chirped pump laser indicates that a chirp of 2.5×10^{15} Hz/s could raise, by an order of magnitude, the SBS threshold of a 20-m fiber. A diode laser with a constant output power and a linear chirp of 5×10^{15} Hz/s has been previously demonstrated. In a low-power proof-of-concept experiment, the threshold for SBS in a 6-km fiber is increased by a factor of 100 with a chirp of 5×10^{14} Hz/s. A linear chirp will enable straightforward coherent combination of multiple fiber amplifiers, with electronic compensation of path length differences on the order of 0.2 m.

©2012 Optical Society of America

OCIS codes: (060.2320) Fiber optics amplifiers and oscillators; (190.5890) Scattering, stimulated; (140.3518) Lasers, frequency modulated.

References and links

1. D. Taverner, D. J. Richardson, L. Dong, J. E. Caplen, K. Williams, and R. V. Penty, "158-μJ pulses from a single-transverse-mode, large-mode-area erbium-doped fiber amplifier," *Opt. Lett.* **22**(6), 378–380 (1997).
2. L. Yingfan, L. Zhiwei, D. Yongkang, and L. Qiang, "Research on stimulated Brillouin scattering suppression based on multi-frequency phase modulation n," *Chin. Opt. Lett.* **7**, 29–31 (2009).
3. D. Brown, M. Dennis, and W. Torruellas, "Improved phase modulation for SBS mitigation in kW-class fiber amplifiers," *SPIE Photonics West*, San Francisco, CA, 24 Jan. 2011.
4. J. Edgecumbe, T. Ehrenreich, C.-H. Wang, K. Farley, J. Galipeau, R. Leveille, D. Björk, I. Majid, and K. Tankala, "kW class, narrow-linewidth, counter pumped fiber amplifiers," *Solid State and Diode Laser Technical Review*, 17 June 2010.
5. I. Dajani, C. Zeringue, C. Lu, C. Vergien, L. Henry, and C. Robin, "Stimulated Brillouin scattering suppression through laser gain competition: scalability to high power," *Opt. Lett.* **35**(18), 3114–3116 (2010).
6. Model YLS-10000-SM, IPG Photonics.
7. K. Shiraki, M. Ohashi, and M. Tateda, "Suppression of stimulated Brillouin scattering in a fibre by changing the core radius," *Electron. Lett.* **31**(8), 668–669 (1995).
8. C. Robin, I. Dajani, and F. Chiragh, "Experimental studies of segmented acoustically tailored photonic crystal fiber amplifier with 494 W single-frequency output," *Proc. SPIE* **7914**, 79140B, 79140B-8 (2011).
9. C. G. Carlson, R. B. Ross, J. M. Schafer, J. B. Spring, and B. G. Ward, "Full vectorial analysis of Brillouin gain in random acoustically microstructured photonic crystal fibers," *Phys. Rev. B* **83**(23), 235110 (2011).
10. S. Gray, D. T. Walton, X. Chen, J. Wang, M.-J. Li, A. Liu, A. B. Ruffin, J. A. Demeritt, and L. A. Zenteno, "Optical fibers with tailored acoustic speed profiles for suppressing stimulated Brillouin scattering in high-power, single-frequency sources," *IEEE J. Sel. Top. Quantum Electron.* **15**(1), 37–46 (2009).
11. G. D. Goodno, S. J. McNaught, J. E. Rothenberg, T. S. McComb, P. A. Thielen, M. G. Wickham, and M. E. Weber, "Active phase and polarization locking of a 1.4 kW fiber amplifier," *Opt. Lett.* **35**(10), 1542–1544 (2010).
12. DARPA ADHELs contract No. HR0011-060C-0029, final report (2008).
13. W. Liang, N. Satyan, A. Yariv, A. Kewitsch, G. Rakuljic, F. Aflatouni, H. Hashemi, and J. Ungar, "Coherent power combination of two master-oscillator-power-amplifier (MOPA) semiconductor lasers using optical phase lock loops," *Opt. Express* **15**(6), 3201–3205 (2007).
14. W. Liang, N. Satyan, A. Yariv, A. Kewitsch, and G. Rakuljic, "Tiled-aperture coherent beam combining using optical phase-lock loops," *Electron. Lett.* **44**(14), 875–876 (2008).

15. N. Satyan, W. Liang, F. Aflatouni, A. Yariv, A. Kewitsch, G. Rakuljic, and H. Hashemi, "Phase-controlled apertures using heterodyne optical phase-locked loops," *IEEE Photon. Technol. Lett.* **20**(11), 897–899 (2008).
16. N. Satyan, W. Liang, A. Kewitsch, G. Rakuljic, and A. Yariv, "Coherent power combination of semiconductor lasers using optical phase-lock loops," *IEEE J. Sel. Top. Quantum Electron.* **15**(2), 240–247 (2009).
17. N. Satyan, A. Vasilyev, G. Rakuljic, V. Leyva, and A. Yariv, "Precise control of broadband frequency chirps using optoelectronic feedback," *Opt. Express* **17**(18), 15991–15999 (2009).
18. V. Lanticq, S. Jiang, R. Gabet, Y. Jaouën, F. Taillade, G. Moreau, and G. P. Agrawal, "Self-referenced and single-ended method to measure Brillouin gain in monomode optical fibers," *Opt. Lett.* **34**(7), 1018–1020 (2009).
19. O. Terra, G. Grosche, and H. Schnatz, "Brillouin amplification in phase coherent transfer of optical frequencies over 480 km fiber," *Opt. Express* **18**(15), 16102–16111 (2010).
20. N. Satyan, G. Rakuljic, and A. Yariv, "Chirp multiplication by four wave mixing for wideband swept-frequency sources for high resolution imaging," *J. Lightwave Technol.* **28**(14), 2077–2083 (2010).
21. J. B. Coles, B. P.-P. Kuo, N. Alic, S. Moro, C.-S. Bres, J. M. C. Boggio, P. A. Andrekson, M. Karlsson, and S. Radic, "Bandwidth-efficient phase modulation techniques for stimulated Brillouin scattering suppression in fiber optic parametric amplifiers," *Opt. Express* **18**(17), 18138–18150 (2010).
22. S. J. Augst, T. Y. Fan, and A. Sanchez, "Coherent beam combining and phase noise measurements of ytterbium fiber amplifiers," *Opt. Lett.* **29**(5), 474–476 (2004).
23. N. Satyan, A. Vasilyev, G. Rakuljic, J.O. White, and A. Yariv, manuscript submitted for publication.
24. D. Brown, M. Dennis, and W. Torruellas, "Improved phase modulation for SBS mitigation in kW-class fiber amplifiers," *Photonics West*, 24 Jan. 2011.

1. Introduction

Stimulated Brillouin scattering (SBS) is a major factor limiting the output power of a fiber laser. In a lossless, passive fiber, SBS occurs when the product of fiber length, L , intensity, I , and Brillouin gain reaches a threshold value. The intensity can be approximated by $I = P/A$, where P is the incident laser power and A is the mode area. We denote by g_0 the gain experienced by a Stokes wave on line center, in the case of a narrowband laser. If the laser linewidth, $\Delta\nu_L$, is large compared to the Brillouin linewidth, $\Delta\nu_B$, the Brillouin gain is given approximately by $g_{\text{eff}} = g_0 \Delta\nu_B / \Delta\nu_L$. Techniques to suppress SBS while maintaining fundamental mode operation include increasing the mode area while reducing the numerical aperture [1], increasing $\Delta\nu_L$ via phase modulation [2–4], laser gain competition [5], and using highly doped fibers to absorb the pump light in a short length to minimize L . A combination of these techniques has yielded 10 kW from a single-mode fiber master oscillator power amplifier [6]. However, the ~2-THz output bandwidth implies that to coherently combine multiple amplifiers, path lengths will have to be matched to ~10 μm .

In this paper, we show that a laser with a linear frequency chirp on the order of 10^{15} Hz/s can suppress, by an order of magnitude, the SBS in a high power fiber amplifier. In addition, it will allow coherent combination of multiple amplifiers and electronic compensation of path length differences on the order of 0.2 m. As a proof of principle, we demonstrate a factor of 100 suppression of the SBS gain in a 6-km fiber, with a chirp of 5×10^{14} Hz/s.

SBS is also a limiting factor in long-distance fiber telecommunications. SBS has been suppressed by a factor of 2.3 in a 14-km fiber by tapering the core from 8 to 7 μm , which varied the Stokes shift by 49 MHz [7]. Varying the core diameter is not an option for high power fiber lasers, because the Stokes shift in a large 30- μm core has a negligible dependence on diameter. Instead, photonic crystal fibers have recently been made with a radially segmented core that flattens the Brillouin gain [8]. Random acoustically microstructured fibers [9] and acoustic anti-guiding fibers [10] have also been shown to reduce the peak SBS gain. The method we propose here will work in conjunction with these fibers.

Recently, two ytterbium (Yb) fiber amplifiers were actively phase locked to a common oscillator, but the 25-GHz oscillator bandwidth means that the amplifier path lengths have to be *mechanically* matched to ~1 mm [11]. The advantage of our seed with a well-defined linear chirp is that path length differences can be *electronically* compensated with an acousto-optic frequency shifter controlled by an optoelectronic phase locked loop. Similar optical

phase-locked loops have already been developed to coherently combine multiple (non-chirped) diode lasers [12–16].

2. Theory

Consider a laser wave at frequency ν_L propagating in the $+z$ direction in a fiber, amplifying a counter-propagating Stokes wave consisting of a superposition of frequencies, ν , that are independent in the undepleted pump regime. For homogeneous broadening, the steady-state Brillouin gain has a Lorentzian frequency dependence with a maximum at $\nu_L - \Omega$ and a full width at half maximum of $\Delta\nu_B$:

$$g(\nu) = \frac{g_0}{1 + \left(\frac{\nu - \nu_L + \Omega}{\Delta\nu_B / 2} \right)^2}, \quad (1)$$

where Ω is the Stokes shift. A linearly chirped laser beam can be represented by

$$\nu_L(z, t) = \nu_0 + \beta \left(t + \frac{L - z}{c/n} \right), \quad (2)$$

where β is the chirp rate. We use $n = 1.45$ for the refractive index. In the presence of a chirp, the situation will be dynamic, but for chirps less than the square of the phonon lifetime, we expect (1) to be a good description of the interaction (see the Appendix). In this case, each frequency component of the counter-propagating Stokes wave will experience a gain given by

$$g(\delta, z) = \frac{g_0}{1 + \left(\frac{\delta - 2\beta n(L - z)/c}{\Delta\nu_B / 2} \right)^2}, \quad (3)$$

where δ is the offset from resonance, i.e. $\delta = \nu - \nu_0 + \Omega$. $g(z)$ is plotted in Fig. 1 for the case $L = 17.5$ m, i.e., a 15-m amplifier followed by a 2.5-m delivery fiber, $\Delta\nu_B = 20$ MHz, and several values of the chirp. A Stokes frequency starting on resonance, i.e., with $\delta = 0$, will experience a gain that decreases with propagation in the $-z$ direction as it moves away from resonance (dashed line in Fig. 1). For $\beta > 0$, a Stokes frequency with $\delta > 0$ will initially see an increase in gain, then a maximum at resonance with the pump, followed by a decrease (solid lines in Fig. 1). The frequency that experiences the largest net gain over the length of the fiber will be offset from resonance by $\delta_{\text{opt}} = \beta\tau$, where τ is the transit time of the fiber, and it will have its peak gain at $z = L/2$.

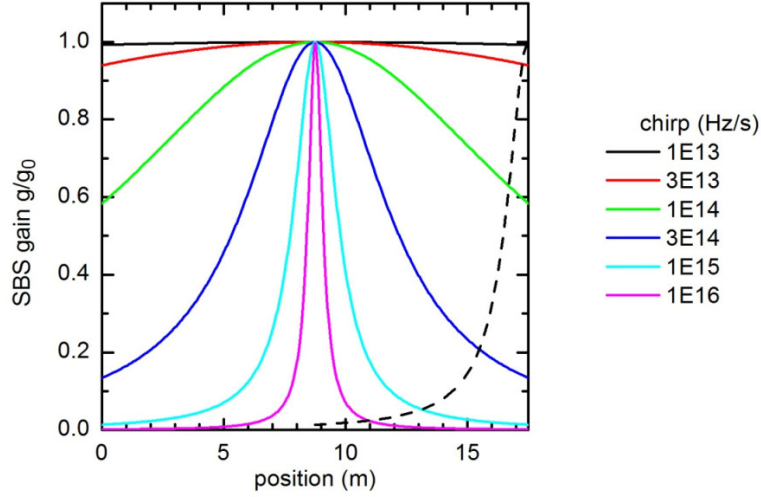


Fig. 1. Normalized SBS gain coefficient vs. position in a 17.5-m fiber, for various chirps and $\Delta\nu_B = 20$ MHz. The Stokes wave propagates from $z = L$ to $z = 0$. The dashed line shows the gain for a chirp of 10^{15} Hz/s, at a Stokes frequency, which is resonant with the laser at $z = L$. The solid lines correspond to the Stokes frequencies that experience the highest integrated gain for each value of the chirp.

In the small-signal regime, for a laser intensity that is uniform in z , each Stokes frequency will experience exponential gain over an effective length given by

$$L_{\text{eff}}(\delta) = \frac{1}{g_0} \int_0^L g(\delta, z) dz = \frac{\Delta\nu_B c}{4n\beta} \left(\tan^{-1} \frac{\delta}{\Delta\nu_B/2} - \tan^{-1} \frac{\delta - 2\beta\tau}{\Delta\nu_B/2} \right). \quad (4)$$

For $\beta \rightarrow 0$, L_{eff} reduces to L . For a large chirp, $L_{\text{eff}} \rightarrow \pi\Delta\nu_B c / 4n\beta$. L_{eff} is shown in Fig. 2 for two values of $\Delta\nu_B$ and two values of L , at δ_{opt} , i.e., the worst-case scenario for the amplifier. For $\Delta\nu_B = 20$ MHz and $L = 17.5$ m, the maximum SBS gain is reduced by a factor of six for a chirp of 10^{15} Hz/s and by a factor of 60 for $\beta = 10^{16}$ Hz/s.

An important feature of this scheme is that long delivery fibers can be accommodated. As an example, for $\Delta\nu_B = 20$ MHz, and $\beta = 10^{15}$ Hz/s, the effective length at δ_{opt} equals 3 m for both a 17.5-m fiber and a 35-m fiber. Once the chirp has reduced L_{eff} to a fraction of L , doubling the fiber length does not increase the net Brillouin gain.

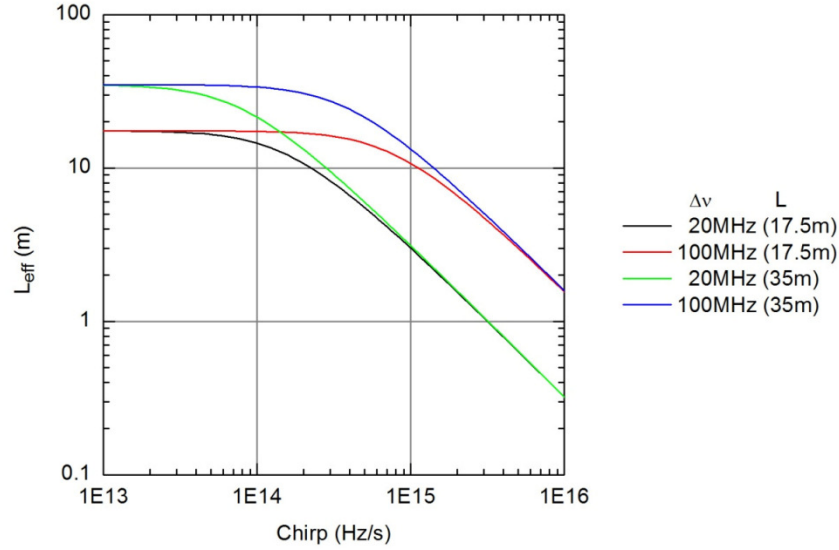


Fig. 2. Plot of L_{eff} vs. chirp, at δ_{opt} , for several values of $\Delta\nu_B$ and L .

A plot of L_{eff} versus offset (Fig. 3) shows that as the chirp increases the optimum offset increases, the gain at the optimum offset decreases, and the gain bandwidth broadens.

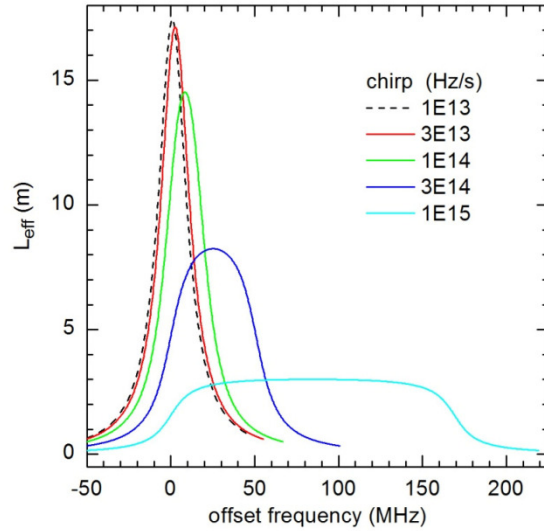


Fig. 3. Plot of L_{eff} vs. Stokes offset frequency, for $\Delta\nu_B = 20$ MHz and $L = 17.5$ m.

The total power in the Stokes wave can be estimated by integrating the exponential gain over a frequency range of $2\beta\tau + \Delta\nu_B$ centered at δ_{opt} , and assuming a constant seed spectral density,

$$P_B = \rho_{\text{seed}} \int \exp[g_0 I_{\text{pump}} L_{\text{eff}}(\delta)] d\delta. \quad (5)$$

The seed density is given by $\rho_{\text{seed}} = R_B^{\text{sp}} P_{\text{in}} / (2\beta\tau + \Delta\nu_B)$, where R_B^{sp} is the Brillouin reflectivity in the spontaneous regime. Even though the integral of $L_{\text{eff}}(\delta)$ is independent of

β , the Stokes power decreases strongly with chirp because P_B is a nonlinear function of $g_0 I_{\text{pump}} L_{\text{eff}}(\delta)$. We next calculate the threshold as a function of chirp, defining the threshold laser power to be that which yields a Brillouin backscattered power equal to 10^{-4} times the incident laser power, and using $R_B^{\text{sp}} = 10^{-6}$. For a fiber core diameter of $27.5 \mu\text{m}$, $L = 17.5 \text{ m}$, $\Delta\nu_B = 20 \text{ MHz}$, and $g_{\text{eff}} = 0.24 \text{ cm/GW}$, the threshold is independent of chirp below 10^{13} Hz/s and rises by a factor of 35 at $\beta = 10^{16} \text{ Hz/s}$ (Fig. 4). Note also that for chirps above 10^{15} Hz/s , the threshold does not increase even for an 85-m delivery fiber.

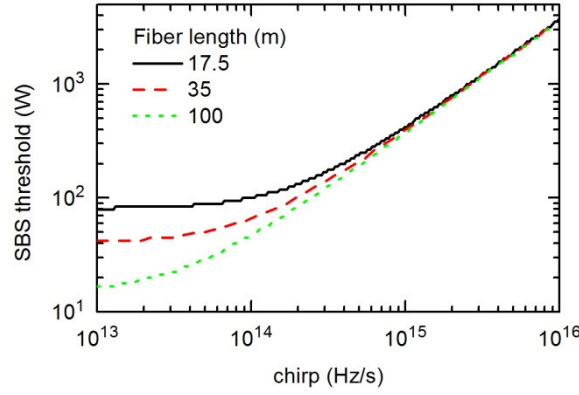


Fig. 4. SBS threshold vs. chirp, for $\Delta\nu_B = 20 \text{ MHz}$ and three different fiber lengths.

3. Experiment

The SBS suppression has been measured by directing a chirped pump beam to a 6-km single mode fiber using a circulator and measuring the reflected power with a photodiode (Fig. 5). The mode field diameter of the fiber is $8 \mu\text{m}$.

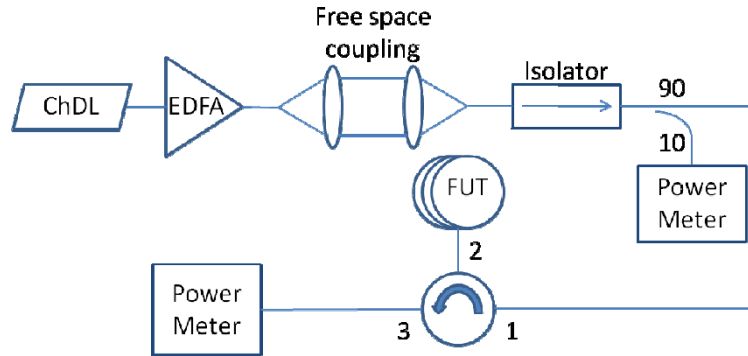


Fig. 5. Experimental layout for observing SBS suppression. A chirped diode laser is amplified in an erbium-doped fiber amplifier and then directed to the fiber under test (FUT) using a circulator.

The seed laser is a $1.5\text{-}\mu\text{m}$ vertical-cavity surface-emitting laser (VCSEL) with a current that is controlled by an optoelectronic phase-locked loop that incorporates a fiber Mach-Zehnder interferometer [17]. The frequency waveform is triangular, with a range of up to 500 GHz and a period as short as $100 \mu\text{s}$. The chirp can be varied between 10^{14} Hz/s and $5 \times 10^{15} \text{ Hz/s}$. The output power is kept constant at 2 mW using a feedback loop that incorporates a semiconductor optical amplifier. The resulting power spectrum is extremely flat (Fig. 6).

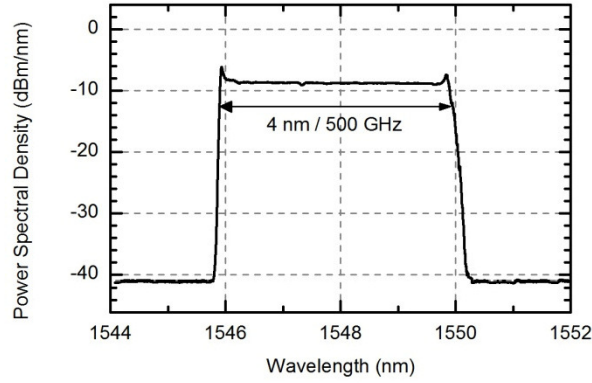


Fig. 6. Power spectrum of the chirped diode laser.

The power reflected from the fiber under test, P_{out} , has contributions from Rayleigh and Brillouin scattering. At each chirp, below the SBS threshold, P_{out} is linearly proportional to P_{in} , indicating that spontaneous Rayleigh scattering is the dominant source (Fig. 7). At zero chirp, the output power rises sharply at the SBS threshold of 20 mW. For a chirp of 10^{14} Hz/s, the threshold increases to 0.4 W. For a chirp of 5×10^{14} Hz/s, the threshold increases to 2 W, clearly establishing the scaling law. The rollover in P_{out} at the higher values of P_B is due to pump depletion.

The solid curves in Fig. 7 are simulations based on (5). The dashed line represents the backscattered Rayleigh power, P_R . We determined the value $P_B / P_R = 1.5 \times 10^{-2}$ below threshold using an optical spectrum analyzer. The value of $g_0 = 5 \times 10^{-12}$ m/W was chosen to fit the zero-chirp data. The Brillouin linewidth $\Delta\nu_B = 110$ MHz was chosen to fit the low chirp data. The simulation curves do not roll over because the calculation made use of the small-signal gain approximation, i.e., it neglects pump depletion.

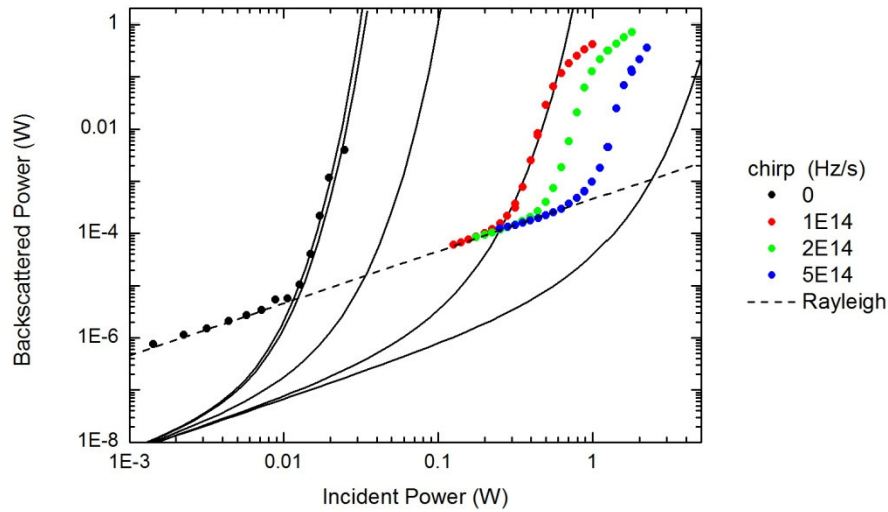


Fig. 7. Backscattered power vs incident power for a 6-km single mode fiber with an 8- μ m mode field diameter. The symbols are the experimental data taken at chirps of $\beta = 0, 10^{14}, 2 \times 10^{14}$, and 5×10^{14} Hz/s. The curves are calculations of the backscattered Brillouin power for $\beta = 10^{11} - 10^{15}$ Hz/s (left to right). The dashed line is the backscattered Rayleigh power.

An independent high-resolution measurement of $\Delta\nu_B$ was made with a distributed feedback laser, balanced photodiode and electronic spectrum analyzer, which allowed us to separate the Rayleigh and Brillouin components [18]. Care was taken to be in the spontaneous regime. The Brillouin spectrum has a width of 39 MHz (Fig. 8), comparable to other recent measurements at 1.5 μm [19].

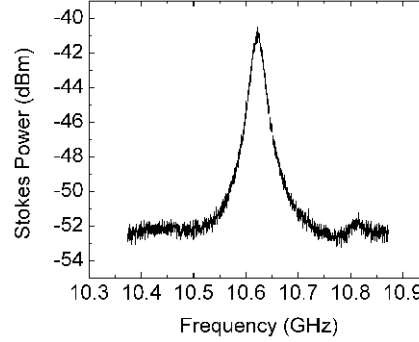


Fig. 8. Spontaneous Brillouin power spectrum for the 6-km single mode fiber.

4. Discussion

This technique has a qualitative resemblance to chirped pulse amplification, wherein pulses are chirped and stretched to lower the intensity and avoid self-focusing in a solid-state amplifier. Here, we are proposing to chirp a continuous wave seed laser to suppress SBS in a fiber amplifier.

If the SBS gain in a 10 – 20 m fiber amplifier turns out to be much broader than the 39-MHz value that we measure for single mode fiber, faster chirps will be required. We believe that through further development of the chirping technique β can be increased to 10^{16} Hz/s to offset an increase in $\Delta\nu_B$. A possible means to achieve linear frequency chirps with even higher chirp rates is by four-wave-mixing [20].

SBS is also a concern in fiber optic parametric amplifiers. When information transmission and signal integrity are important criteria, a frequency-hopped chirp can be used to suppress SBS with high bandwidth-efficiency [21].

The value for g_0 determined from fitting the data in Fig. 7 is a factor of three lower than the value measured in [18] using a different technique. The discrepancy may be due to errors in calibration, the use of acousto-optic effective area in [18], and also the ~30 MHz bandwidth of our unchirped laser. The intrinsic laser bandwidth may also enter into the determination of $\Delta\nu_B$ from fitting the data in Fig. 7. This could explain the discrepancy with the independent measurement in Fig. 8.

For coherent combining of multiple amplifiers, the transient phase variations intrinsic to the fiber amplifier have to be in a frequency range that a phase-locked loop can follow. The power scaling of the phase noise spectrum at the output of a 10-W Yb fiber amplifier [22] suggest that the 1-MHz bandwidth phase-locked loops already developed will be sufficient for multi-kW lasers [13–16].

A major advantage of the linear chirp for coherent combining is that it allows for a straightforward compensation of path length differences by preceding each amplifier with an acousto-optic frequency shifter (AOFS) [23]. The longest path length difference that can be compensated will be limited by several factors. The range of the AOFS will impose a limit of

$$\Delta L_{\max} < \frac{c \Delta\nu_{\max}}{n\beta}. \quad (6)$$

A typical range is $\Delta\nu_{\max} = 10\text{ MHz}$. At a chirp of 10^{15} Hz/s , this would yield $\Delta L_{\max} < 2\text{ m}$. Considering that other factors may enter, a conservative estimate would be $\Delta L_{\max} < 0.2\text{ m}$.

Due to the exponential nature of the Brillouin gain, any variation (or structure) in the spectrum of gIL lowers the SBS threshold. Sinusoidal phase modulation of a narrowband laser introduces side bands, giving the Brillouin gain spectrum a high peak-to-average ratio. Large amplitude phase modulation of the laser via pseudo-random bit sequences is one attempt to flatten the gain spectrum [24]. A salient characteristic of the linear chirp is the uniformity of the Stokes gain spectrum (Figs. 3, 6). This means that a tenfold increase of the SBS threshold of a 17.5-m fiber can be obtained with a chirp of $2.5 \times 10^{15}\text{ Hz/s}$ (Fig. 4), which would broaden the effective gain spectrum to only 340 MHz, as compared to the $\sim 3\text{ GHz}$ bandwidth required when using phase modulation [4].

5. Conclusion

Our analysis shows that a linearly chirped diode laser seed has the potential to significantly suppress the SBS that is currently limiting the output power of narrow-linewidth fiber amplifiers. Experiments at $\sim 3\text{ W}$ with a passive 6-km fiber are in agreement with estimates based on a simple model. Extrapolating to a 17.5-m fiber and 20-MHz Brillouin bandwidth, we anticipate a factor of ~ 20 increase in SBS threshold for a chirp of $5 \times 10^{15}\text{ Hz/s}$.

Appendix

The purpose of the following analysis is to estimate the maximum chirp for which (1) would be a useful estimate of the interaction between a chirped laser and Stokes wave. In the slowly varying envelope approximation, we expect the interaction within a single mode fiber to be described by coupled partial and ordinary differential equations for the envelopes of the laser field, E_L , the Stokes field, E_S , and the acoustic wave amplitude ρ [25]. Consider a short length of fiber within which E_L and E_S are known. In regions of the fiber where the contribution of thermal phonons can be neglected, the system of equations reduces to

$$\frac{d\rho}{dt} = -\frac{\rho}{\tau} + i\Lambda E_L E_S^* \exp(i\pi\beta t^2), \quad (7)$$

where a phase equal to the integral of the chirp has been added to E_L . Here τ is the phonon decay time, and Λ is the acoustic coupling parameter. We numerically integrate (7) over the interval $t = -10/\tau\beta$ to $t = 10/\tau\beta$, with the initial condition $\rho = 0$. The solution is then normalized to the phase of the laser field, and to the magnitude of the steady-state solution in the absence of chirp, i.e., we consider $\rho_n = \rho \exp(-i\pi\beta t^2) / \Lambda E_L E_S^*$. For each chirp, time t can then be re-scaled to frequency ν_s using (2). ν represents the offset from resonance, i.e. $\nu = \nu_L - \nu_s - \Omega$. Therefore, $\rho(\nu)$ represents the response of the medium in the neighborhood of resonance, given that the laser field is in the middle of a frequency sweep. The exponential gain coefficient $g(\nu)$ is proportional to the imaginary part of ρ_n (Fig. 9), which has an approximately Lorentzian shape even at $3 \times 10^{15}\text{ Hz/s}$. This confirms our expectation that the steady state gain in (1) would be useful up to chirps approximately equal to the Brillouin bandwidth squared. We note here that the integral of $\text{Im}(\rho)$ is independent of chirp.

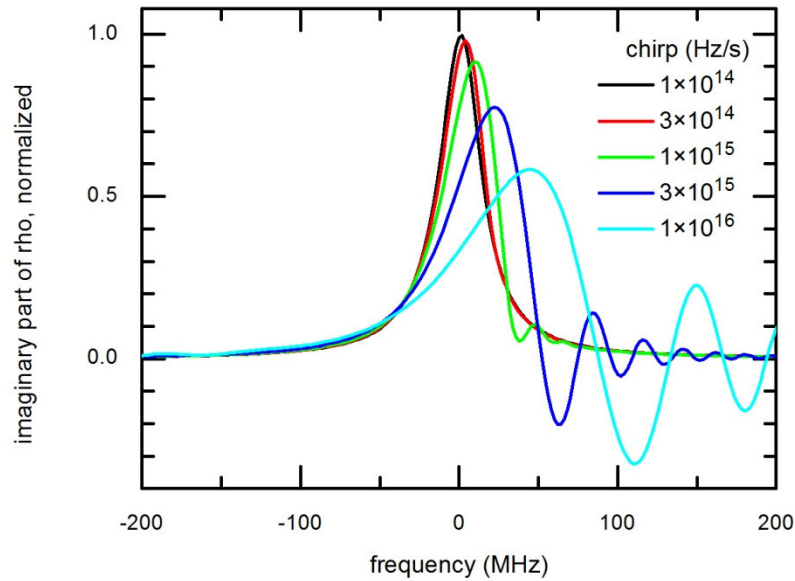


Fig. 9. Frequency dependence of $\text{Im}(\rho)$, normalized to the zero-chirp steady-state value, for different values of the chirp, and $\tau = 10$ ns.

Acknowledgments

This work has been supported by High Energy Laser Joint Technology Office contract 11-SA-0405. We are also grateful for continuing technical input from Scott Christensen, John Edgecumbe, and Imtiaz Majid at Nufern.